J. Fluid Mech. (2006), *vol.* 558, *pp.* 309–318.
doi:10.1017/S0022112006000206 Printed in the United Kingdom

Sustained sub-laminar drag in a fully developed channel flow

By TAEGEE MIN, SUNG MOON KANG, JASON L. SPEYER AND JOHN KIM

Department of Mechanical and Aerospace Engineering, University of California, Los Angeles, CA 90095-1597, USA

(Received 13 February 2006 and in revised form 23 March 2006)

It is shown, by direct numerical simulations, that the skin-friction drag in a fully developed channel can be sustained below that corresponding to the laminar profile when the flow is subjected to surface blowing and suction in the form of an upstream travelling wave. A key mechanism that induces the sub-laminar drag is the creation of positive (negative) Reynolds shear stress in the wall region, where normally negative (positive) Reynolds shear stress is expected given the mean shear. This mechanism is contained in the linearized Navier–Stokes equations, thus allowing linear analysis of the observed phenomena. When applied to a fully developed turbulent channel flow, skin-friction drag is also significantly reduced by an upstream travelling wave, demonstrating that the surface blowing and suction in the form of such a wave is also effective in fully developed turbulent flows. Consideration of the energy budget shows a possibility of net drag reduction in turbulent channel flows with the present open-loop control.

1. Introduction

The minimum sustainable drag in a fully developed channel (pipe) flow is of fundamental importance, as it can be used as a basis for performance limitations for various controllers designed to reduce skin-friction drag in channel (pipe) flow. Bewley (2001, see also Bewley & Aamo 2004) proposed the following conjecture ('Bewley's conjecture' hereinafter):

> "The lowest sustainable drag of an incompressible constant mass-flux channel flow, when controlled via a distribution of zero-net mass-flux blowing/suction over the no-slip channel walls, is exactly that of the laminar flow."

This conjecture can be elucidated by a useful expression for skin-friction drag in fully developed channel flows (Fukagata, Iwamoto & Kasagi 2002 and Bewley & Aamo 2004):

$$D = \frac{1}{2}\left(\left.\frac{\mathrm{d}U}{\mathrm{d}y}\right|_{-1} - \left.\frac{\mathrm{d}U}{\mathrm{d}y}\right|_{1}\right) = 2 + \frac{3}{2}Re\int_{-1}^{1}\overline{u'v'}y\,\mathrm{d}y. \tag{1.1}$$

Here, all quantities are normalized by the centreline velocity of the laminar Poiseuille flow ($U_c = \frac{3}{2}U_b$, U_b is the bulk velocity) and the channel half-height (δ), U denotes the mean velocity, Re the Reynolds number based on the laminar centreline velocity, and $\overline{u'v'}$ is the Reynolds shear stress. In this paper, u, v, and w denote, respectively, the velocity component in the streamwise (x), wall-normal (y), and spanwise (z) directions, and the prime denotes a fluctuating quantity. Note that (1.1) is valid for all channel flows with the same mass flux as the base laminar flow (4/3 with the

present normalization). The first term on the right-hand side of (1.1) represents the mean wall-shear rate of laminar flow ($U = 1 - y^2$), and therefore (1.1) shows that skin-friction drag in a channel flow consists of the laminar drag plus the y-weighted integral of $\overline{u'v'}$. From the viewpoint of (1.1), Bewley's conjecture is equivalent to saying that the y-weighted integral of $\overline{u'v'}$, with and without control input, is always positive in channel flows. For regular channel flows without control, this is the case, since the Reynolds shear stress in the lower half of the channel ($-1 < y < 0$) is negative, while the opposite is true in the upper half of the channel ($0 < y < 1$). As such, the skin-friction drag in transitional and turbulent channel flows is higher than that of the corresponding laminar flow with the same mass flux. With a form of periodic control, Bewley & Aamo (2004) report that they could not sustain the Reynolds shear stress necessary to yield drag below the laminar value. They provide phenomenological justification by a Reynolds analogy between convective momentum transport and convective heat transport, but they left the proof of the conjecture as an open problem.

The objective of this paper is to explore a control input, in the form of zero-net-mass-flux blowing and suction on the wall, that can sustain the Reynolds shear stress in such a way that the y-weighted integral of $\overline{u'v'}$ remains negative. In the following sections, we shall show that a control input in the form of an upstream travelling wave indeed produces the Reynolds shear stress that makes a negative contribution to the total drag, resulting in sustained sub-laminar drag in a fully developed channel flow. It is worth pointing out that although control input in the form of surface blowing and suction used in the present work is easy to implement numerically, it may not be straightforward to implement in real flows. An alternative possibility is discussed in § 5.

2. Linear analysis

Recent studies have shown that certain linear mechanisms play important roles in turbulent boundary layers (for example, see Jiménez & Pinelli 1999; Kim & Lim 2000). Recognizing the role of linear mechanisms, particularly that of self-sustaining near-wall turbulence in turbulent boundary layers, several investigators have successfully applied modern control theories to develop optimal controllers based on the linearized Navier–Stokes equations (see, for example, Bewley 2001 and Kim 2003 and references therein). The success of these controllers when applied to fully nonlinear flows further demonstrates the usefulness of linear analysis in designing controllers for fully nonlinear flows. Here, we first study the effect of travelling control waves on the Reynolds shear stress by examining the solution to the linearized Navier–Stokes equations.

The linearized Navier–Stokes equation for a two-dimensional channel flow can be written as

$$\frac{\partial \hat{v}}{\partial t} = (\nabla^2)^{-1}\left(-\mathrm{i}\alpha U \nabla^2 + \mathrm{i}\alpha \frac{\mathrm{d}^2 U}{\mathrm{d}y^2} + \frac{1}{Re}\nabla^4\right)\hat{v}, \tag{2.1}$$

where $\hat{v}$ denotes the Fourier-transformed wall-normal velocity perturbation (v'), $\nabla^2 = \partial^2/\partial y^2 - \alpha^2$, and α is a wavenumber in the streamwise direction. Equation (2.1) can be written in the following state-space representation (for further details, see Kim 2003):

$$\frac{\mathrm{d}\boldsymbol{x}}{\mathrm{d}t} = \boldsymbol{A}\boldsymbol{x} + \boldsymbol{B}\boldsymbol{u}, \tag{2.2}$$

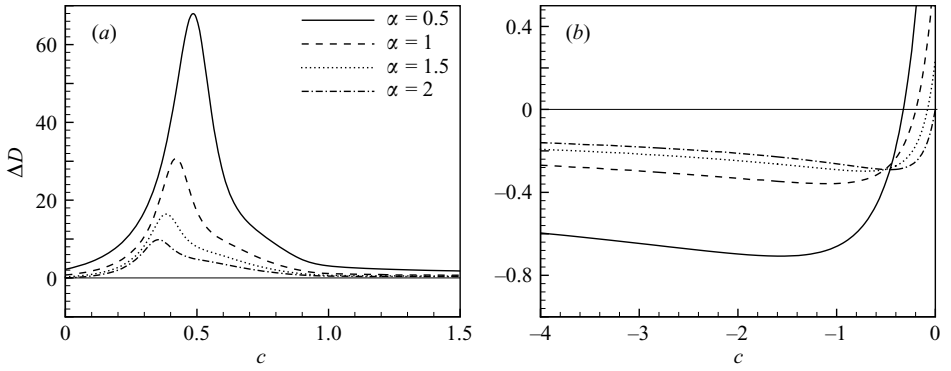

FIGURE 1. ΔD in steady state at $Re = 2000$ and $a = 0.1$: (a) downstream travelling waves ($c > 0$); (b) upstream travelling waves ($c < 0$).

where the vector $\boldsymbol{x}$ represents the 'state' of the system and consists of $\hat{v}$ in Galerkin-Chebyshev space. The system matrix $\boldsymbol{A}$ is related to the linear operator in (2.1), while the input matrix $\boldsymbol{B}$ and the control $\boldsymbol{u}$ determine how the control input affects the state. For any control $\boldsymbol{u}$, the solution to equation (2.2) can be found by:

$$\boldsymbol{x}(t) = \mathrm{e}^{\boldsymbol{A}t}\boldsymbol{x}(0) + \int_0^t \mathrm{e}^{\boldsymbol{A}(t-\tau)}\boldsymbol{B}\boldsymbol{u}(\tau)\,\mathrm{d}\tau. \tag{2.3}$$

We consider the solution when control input is introduced as surface blowing and suction in the form of a travelling wave. The initial objective of this study was to develop a control strategy for viscous drag reduction through periodic control of a turbulent boundary layer. In the process of optimizing the control input defined at multiple wavenumbers, it was observed that certain upstream travelling waves reduced the drag, while certain downstream travelling waves increased the drag. In order to simplify our analysis, we consider travelling control waves consisting of a single wavenumber. Such a control can be expressed in physical space as boundary conditions for v:

$$v_{\mathrm{w}} = a\cos(\alpha(x - ct)), \tag{2.4}$$

where a and c denote the amplitude and wave speed of blowing/suction on the wall, respectively. In the present study, the blowing/suction (2.4) is implemented on both walls in varicose mode, i.e. the upper and lower walls have the blowing/suction in phase at the same streamwise locations. Note that, with stable systems, $\exp(\boldsymbol{A}t) \to 0$ as $t \to \infty$. Given control input (2.4), equation (2.3) can be analytically solved for $\hat{v}$ as $t \to \infty$, and the Reynolds shear stress ($\overline{u'v'}$) is obtained using the continuity equation ($\mathrm{i}\alpha\hat{u} + \partial\hat{v}/\partial y = 0$).

Figure 1 shows the y-weighted integral of $\overline{u'v'}$ as a function of the wave speed for $Re = 2000$ and $a = 0.1$. Here, ΔD is defined as

$$\Delta D = \frac{3}{2}Re\int_{-1}^{1}\overline{u'v'}\,y\,\mathrm{d}y. \tag{2.5}$$

Note that ΔD is positive (increased drag) with downstream travelling waves ($c > 0$), whereas it is negative (reduced drag) with upstream travelling waves ($c < 0$) except near small negative c (slow upstream travelling wave). Note also that there exists an optimal wave speed, where ΔD reaches its minimum (with negative c) and maximum (with positive c). We mention in passing that the large peak with a positive c is

related to the most observable and controllable system mode. Also, although this large production of ΔD at a certain c is of no interest to the present study, it can be useful in certain applications and warrants further study.

It is apparent from the linear analysis that certain surface blowing and suction in the form of an upstream travelling wave can induce the Reynolds shear stress in such a way that the total drag could be less than that of the laminar flow. This is contrary to Bewley's conjecture. Strictly speaking, however, the linear analysis assumes that the mean velocity profile, and hence the drag, is not affected by perturbations (i.e. the system matrix $\boldsymbol{A}$ is independent of $\boldsymbol{x}$). The real effect of travelling waves on the drag must be investigated by a direct numerical simulation, where the nonlinear effects are included. In the following section, we begin investigating whether such Reynolds shear stress can be sustained in nonlinear flows with the same control input.

Bewley & Aamo (2004) provided a phenomenological justification by an analogy between convective momentum transport and convective heat transport. Clearly, this analogy does not hold. This failure of the analogy, however, is not due to nonlinearity of momentum transport since the present analysis is linear. Rather, it is due to differences in the linear equations. Among others, convective heat transport is governed by a single scalar equation, whereas convective momentum transport is governed by two equations coupled through the continuity equation. The present linear analysis indicates that a certain flow-field unsteadiness induced by wall-normal motion can decelerate the momentum transport in the direction of viscous diffusion, whereas the heat transport is always accelerated by flow-field unsteadiness as pointed out by Bewley & Aamo (2004).

3. Two-dimensional channel flow

We will first study the effect of travelling waves in two-dimensional channel flows. Disturbances are finite but they are two-dimensional, similar to those considered by Bewley & Aamo (2004). A pseudo-spectral code similar to that used by Kim, Moin & Moser (1987) is employed. Simulations are conducted at $Re = 2000$, and the computational domain of $4\pi\delta \times 2\delta$ is used in the streamwise and wall-normal directions, respectively, with a 32×65 grid. The mean pressure gradient is varied to maintain a constant mass flux, and the total drag is measured by averaging the mean velocity gradient on both walls.

Figure 2 shows the results for a travelling wave of $\alpha = 0.5$ at $c = -2$. All simulations start from the laminar flow with no initial disturbances, and a steady state is reached when $t > 500$ as shown in figure 2(a). It is apparent that the sub-laminar drag is sustained for all amplitudes shown. Figure 2(b) shows that the results from the linear analysis agree with those from direct numerical simulations for small amplitudes. As expected, the nonlinear results deviate from the linear solutions as the amplitude is increased (figure 2b).

In order to examine the physical mechanism responsible for drag reduction by the upstream travelling waves, we performed numerical simulations of 'channel flow' without the imposed mean flow, i.e. $U = 0$ everywhere initially and the imposed mean pressure gradient was set to zero. Blowing and suction as prescribed in (2.4) was applied, and the simulations were carried out until a statistically steady state was reached. The momentum balance for this flow is

$$\frac{\mathrm{d}}{\mathrm{d}y}\left(-\overline{u'v'} + \frac{1}{Re}\frac{\mathrm{d}U}{\mathrm{d}y}\right) = 0 \quad \text{or} \quad -\overline{u'v'} + \frac{1}{Re}\frac{\mathrm{d}U}{\mathrm{d}y} = C. \tag{3.1}$$

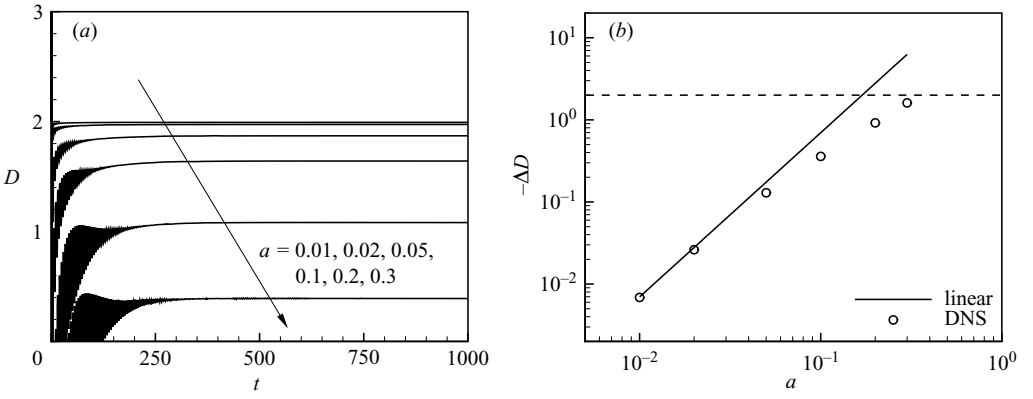

FIGURE 2. Viscous drag in a two-dimensional channel flow with $\alpha = 0.5$ and $c = -2$: (*a*) time histories of D for various control amplitudes; (*b*) ΔD in a steady state as a function of control amplitudes.

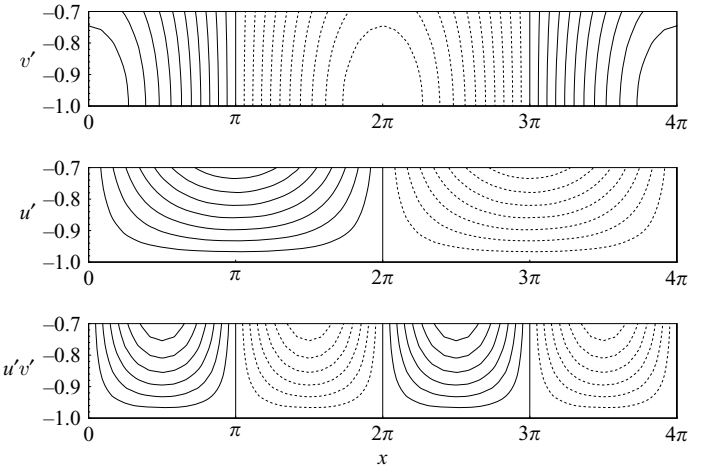

FIGURE 3. Contours of v' (top), u' (middle) and $u'v'$ (bottom) near the lower wall with a standing wave. Contour levels for v', u' and $u'v'$ are −0.01–0.01, −0.02–0.02 and −0.0001–0.0001, respectively (20 levels).

The integration constant C must be zero to satisfy the boundary conditions. A standing wave ($c = 0$ in (2.4)) created no net $-\overline{u'v'}$ as expected from the symmetry of the problem. Upstream travelling waves created positive $\overline{u'v'}$ near the lower wall, which was balanced by a positive $\mathrm{d}U/\mathrm{d}y$, implying that U is positive. In other words, upstream travelling waves induced a net mass flux in the opposite direction. Downstream travelling waves would create the opposite effect due to the apparent symmetry. The amount of induced mass flux was proportional to the amplitude of the travelling wave. Contours of v', u', and $u'v'$ near the lower wall with a standing wave and an upstream-travelling wave are shown in figures 3 and 4, respectively. It is apparent that the travelling wave had a different impact on the phase of u' and v'. Figure 5 illustrates the effect of standing and travelling waves on u' and v' at a location near the lower wall ($y = -0.95$) at $\omega t = 2\pi$. With a standing wave, the phase of u', which is related to that of $\mathrm{d}v'/\mathrm{d}y$ through the continuity equation, is 90° out

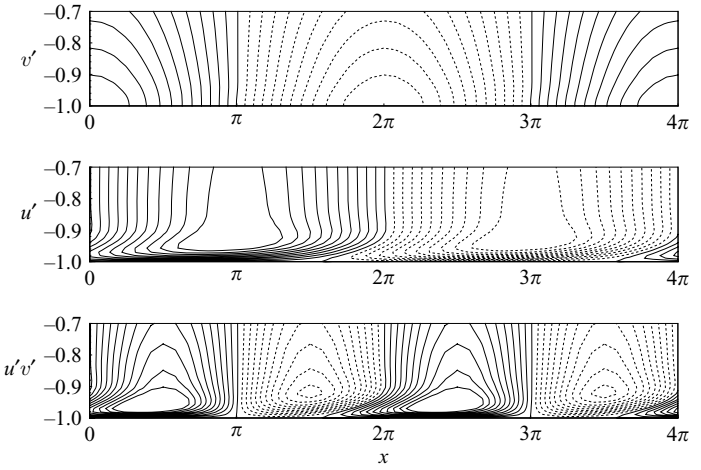

FIGURE 4. Contours of v' (top), u' (middle) and $u'v'$ (bottom) near the lower wall with an upstream travelling wave. Contour levels are the same as those used in figure 3.

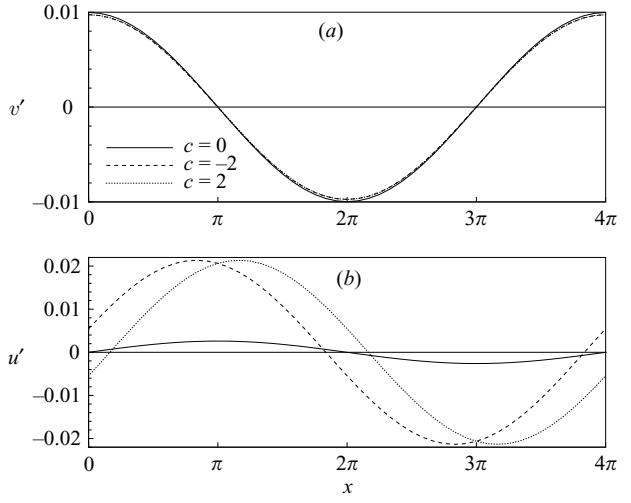

FIGURE 5. Effect of standing and travelling waves on u' and v' at $y = -0.95$ for $Re = 2000$, $\alpha = 0.5$ and $a = 0.01$: (*a*) v'; (*b*) u'.

of phase as shown in the figure. With an upstream travelling wave, the phase of v' remains approximately the same as that of the travelling wave, while that of u' is leading (upstream direction) that of v'. This phase lead in u' results in a net positive Reynolds stress as can be seen from

$$v' = c_1 \cos(\alpha x), \tag{3.2}$$

$$u' = c_2 \sin(\alpha x + \phi), \tag{3.3}$$

$$\overline{u'v'} = c_1 c_2 \overline{\sin(\alpha x + \phi)\cos(\alpha x)} = \tfrac{1}{2} c_1 c_2 \sin\phi. \tag{3.4}$$

With a positive ϕ as shown in figure 5, $\overline{u'v'}$ is positive. With a downstream travelling wave, ϕ is negative, resulting in a negative $\overline{u'v'}$. This phase shift in u' resulted in net

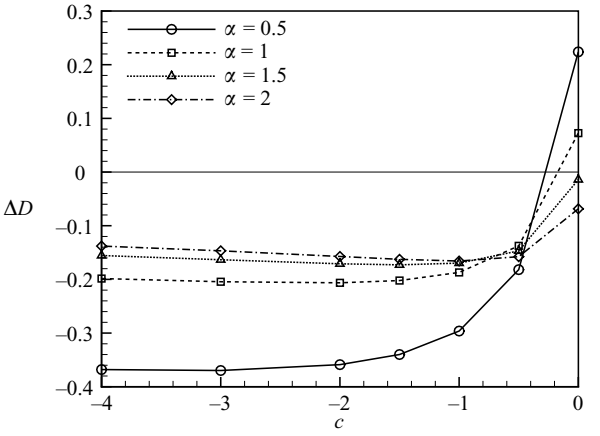

FIGURE 6. ΔD as a function of the wave speed and wavenumber for $a = 0.1$.

positive (negative) Reynolds shear stress with an upstream (downstream) travelling wave, which in turn induced net mass flux in the direction opposite to the travelling wave. The effect of travelling waves in a channel flow would be similar, although it would have been modified by the presence of mean U driven by the mean pressure gradient. Since an upstream travelling wave induces a net mass flux in the streamwise direction, the amount of mass flux to be driven by the pressure gradient in the channel flow with a fixed mass flux is reduced, resulting in reduced drag. If we had fixed the mean pressure gradient instead, the net mass flux in the channel would have increased due to the positive mass flux induced by an upstream travelling wave.

The flow remains stable for large a as the drag continues to decrease. However, when the amplitude exceeds a certain value, the induced mass flux exceeds the fixed mass flux. In fact, the drag (and hence the pressure force required to maintain the same mass flux) becomes negative as the entire flow is driven by the power required to provide the blowing and suction, and comparison with a channel flow is no longer meaningful. With downstream travelling waves ($c > 0$), on the other hand, the flow becomes unstable and the drag increases drastically as a is increased.

Figure 6 shows drag variations as a function of the wave speed for different streamwise wavenumbers with a fixed amplitude $a = 0.1$. Note that ΔD in nonlinear simulations represents the change in the total drag (see equation (1.1)). The nonlinear results show the same trend observed in the linear solutions: that is, ΔD becomes larger for smaller α, and there is an optimal wave speed that induces the minimum ΔD. The optimal wave speed for nonlinear simulations appears to be slightly more negative (faster upstream) than that of the linear solutions.

4. Turbulent channel flow

In this section, we investigate the effect of travelling waves in a turbulent channel flow. The same code is used to perform direct numerical simulations of a turbulent channel flow at $Re = 2000$. The computational domain is $4\pi\delta \times 2\delta \times 4\pi\delta/3$ in the streamwise, wall-normal and spanwise directions, respectively, and $64 \times 97 \times 64$ grid points are used in each direction. All simulations were started from a turbulent channel flow that had reached a steady state without control input. Figure 7 shows time histories of D in a turbulent channel flow. An upstream travelling wave at $\alpha = 0.5$ with $c = -2$ is applied on both walls in varicose mode, as was the case for the

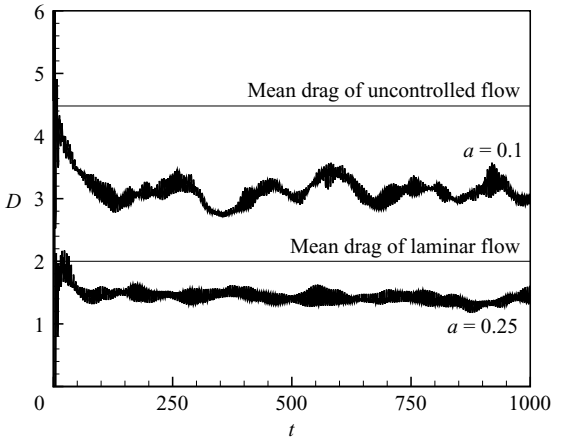

FIGURE 7. Time histories of D in a turbulent channel flow for $\alpha = 0.5$ and $c = -2$.

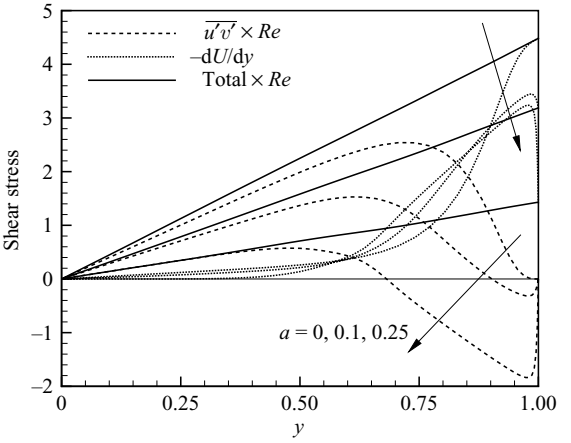

FIGURE 8. Distribution of total, viscous, and Reynolds shear stresses in the upper half of the channel for different control amplitudes. This is for the case of $\alpha = 0.5$ and $c = -2$.

two-dimensional channel discussed in § 3. The same parameters as in two-dimensional channel flow were used, and they are by no means optimal ones for turbulent channel flows. Similar to the two-dimensional flows, a significant drag reduction is obtained, and the reduction is greater for larger amplitudes (about 30 % and 70 % drag reduction, respectively, with amplitudes 0.1 and 0.25). Note that, with $a = 0.25$, the sustained drag is sub-laminar even for this three-dimensional flow. It is worth noting, however, that this amplitude is much larger than that used in the opposition control of Choi, Moin & Kim (1994) and in the LQG control of Lee *et al.* (2001).

Figure 8 shows the total shear stress for the case of $\alpha = 0.5$ and $c = -2$ with $a = 0, 0.1$ and 0.25. The total shear stress for each case is a straight line, indicating that the flow has indeed reached a statistically steady state. Also shown in the figure are viscous stress (dU/dy) and Reynolds shear stress ($\overline{u'v'}$). The positive $\overline{u'v'}$ in uncontrolled turbulent flow (note that only the upper half of the channel is shown in the figure, where the Reynolds shear stress is normally positive) is decreased by the effect of the upstream travelling wave. For the case of $a = 0.25$, $\overline{u'v'}$ near the wall becomes negative, which in turn results in sub-laminar drag.

The efficiency of the present control input in the form of a travelling wave is of great interest. In the present study, the efficiency η is defined as

$$\eta = \frac{P_{\mathrm{drag}} + P_{\mathrm{input}}}{P_0}. \tag{4.1}$$

Here, P_0, P_{drag} and P_{input} denote the power required for uncontrolled flow, the power required for drag-reduced flow, and power input for blowing and suction, respectively, and they can be expressed as

$$P_0 = \frac{4}{3}\frac{1}{Re}D_0, \quad P_{\mathrm{drag}} = \frac{4}{3}\frac{1}{Re}D, \quad P_{\mathrm{input}} = \overline{\left(p_{\mathrm{w}} + \tfrac{1}{2}v_{\mathrm{w}}^2\right)v_{\mathrm{w}}}, \tag{4.2}$$

where D_0 denotes the mean wall-shear rate of uncontrolled flow, and p_{w} and v_{w} are the pressure and wall-normal velocity at the wall, respectively. Recall that the bulk velocity used in defining the power is $2/3$ with the present normalization and the total drag is the sum of the drag on each wall. Also note that additional power required to account for the friction loss associated with blowing and suction through the wall is not included in (4.1). For $a = 0.1$ and $a = 0.25$, the efficiency η was found to be 0.76 and 0.81, respectively. In other words, the total power required to have the same mass flux was only 76% and 81% of the power required in a channel without control. Recall that there was about 30% and 70% drag reduction for $a = 0.1$ and $a = 0.25$, respectively. In comparison, the opposition control of Choi *et al.* (1994) reduced drag in a channel by about 30% and η was found to be about 0.7. For that closed-loop control, P_{input} was negligible compared to P_0, and therefore the power saved is directly related to the reduced drag. For the present open-loop control, however, P_{input} was significant, and the power saved was less (especially for high a) than the saving due to reduced drag. This was in part due to the large amplitudes of the travelling waves. Its low power saving notwithstanding, it is remarkable that substantial drag reduction can be achieved in a turbulent channel flow with such a simple open-loop control.

5. Concluding remarks

Motivated by Bewley's conjecture (Bewley 2001), we investigated the possibility of achieving sub-laminar drag in a fully developed channel flow. Sustainable sub-laminar drag was obtained when the flow was subjected to blowing and suction at the wall in the form of an upstream travelling wave. It was found, both from linear analysis and nonlinear simulations, that certain upstream travelling waves induce the Reynolds shear stress in such a way that it makes a negative contribution to the total viscous drag. This was the case not only for the two-dimensional channel flow considered by Bewley & Aamo (2004), but also for a three-dimensional turbulent channel flow. Note that the Reynolds shear stress induced by upstream travelling waves reduces the production of kinetic energy, and therefore the flow remains stable for large-amplitude upstream travelling waves.

Downstream travelling waves, on the other hand, increase the drag. The linear analysis shows that at certain wave speeds the drag increase is dramatic. There are certain applications where the increase in Reynolds shear stress could be desirable. For example, an optimized downstream travelling wave could be used to prevent or delay separation in turbulent boundary layers subject to a strong pressure gradient (e.g. in a diffuser or flow over an airfoil). The optimal use of downstream travelling waves is something that warrants further study.

The open-loop control presented was discovered serendipitously while exploring periodic control of turbulent boundary layers. Unlike the cyclic application of a

pressure feedback control (turning on and off their 'win-win' mechanism) by Bewley & Aamo (2004), our periodic optimization specifically tasked the wall-normal surface blowing/suction control to return the flow state back to its initial condition. Both the time period of control and initial state were part of the optimization (see Speyer 1996). Numerically calculated gradients were used to find a control history, an initial state, and a time period that minimized viscous drag. The two-dimensional travelling wave was discovered as we simplified the optimization to make the problem more tenable. The control presented in this paper is not an optimal solution; our purpose was to investigate whether a sub-laminar drag can be sustained in a fully developed channel flow. In the light of this new finding, optimization is underway. In particular, we plan to explore control input in the form of spanwise and obliquely travelling waves as well as constructing periodic regulators to form closed-loop solutions.

Finally, the current control scheme, consisting of surface blowing and suction in the form of travelling waves, is mathematically simple (and hence easy to implement in numerical experiments), yet it may not be straightforward to implement in real flows. For example, additional space is required to retain the flow through the walls, and the additional hardware required to control blowing and suction may be complicated. However, a moving surface with wavy motion would produce a similar effect, since wavy walls with small amplitudes can be approximated by surface blowing and suction. We plan to perform simulations over moving wavy walls.

The authors gratefully acknowledge the support provided by the Air Force Office of Scientific Research (F49620-03-1-0244, Dr Heise, program manager) during the course of this work. The computer time provided through the National Science Foundation NRAC program is also gratefully acknowledged.

REFERENCES

Bewley, T. R. 2001 Flow control: new challenges for a new renaissance. *Prog. Aerospace Sci.* **37**, 21–58.

Bewley, T. R. & Aamo, O. M. 2004 A 'win-win' mechanism for low-drag transients in controlled two-dimensional channel flow and its implications for sustained drag reduction. *J. Fluid Mech.* **499**, 183–196.

Choi, H., Moin, P. & Kim, J. 1994 Active turbulence control for drag reduction in wall-bounded flows. *J. Fluid Mech.* **262**, 75–110.

Fukagata, K., Iwamoto, K. & Kasagi, N. 2002 Contribution of Reynolds stress distribution to the skin friction in wall-bounded flows. *Phys. Fluids* **14**, L73–L76.

Jiménez, J. & Pinelli, A. 1999 The autonomous cycle of near-wall turbulence. *J. Fluid Mech.* **389**, 335–359.

Kim, J. 2003 Control of turbulent boundary layers. *Phys. Fluids* **15**, 1093–1105.

Kim, J. & Lim, J. 2000 A linear process in wall-bounded turbulent shear flows. *Phys. Fluids* **12**, 1885–1888.

Kim, J., Moin, P. & Moser, R. D. 1987 Turbulence statistics in fully developed channel flow at low Reynolds number. *J. Fluid Mech.* **177**, 133–166.

Lee, K. H., Cortelezzi, L., Kim, J. & Speyer, J. 2001 Application of reduced-order controller to turbulence flows for drag reduction. *Phys. Fluids* **13**, 1321–1330.

Speyer, J. L. 1996 Periodic optimal flight. *AIAA J. Guidance, Control, Dyn.* **19**, 745–755.